Journal of Classification 16:197-223 (1999)

Shape Statistics: Procrustes Superimpositions and Tangent Spaces

F. James Rohlf

State University of New York at Stony Brook

Abstract: The shape of a set of labeled points corresponds to those attributes of the configuration that are invariant to the effects of translation, rotation, and scale. Procrustes distance may be used to compare different shapes and also serve as a metric that may be used to define multidimensional shape spaces. This paper demonstrates that the preshape space of planar triangles Procrustes aligned to a reference triangle corresponds to a unit hemisphere. An overview of methods used as linear approximations of D. G. Kendall's non-Euclidean shape space is given, and the equivalence of several methods based on orthogonal projections is shown. Some problems with approximations based on stereographic projections are also discussed. A simple example using artificial data is included.

Keywords: Kendall shape space; Preshape space; Tangent space; Partial warps; Multivariate analysis.

The helpful critical comments by Fred L. Bookstein are gratefully acknowledged. The detailed suggestions by Dean Adams through the many revisions of this manuscript were very helpful. Thanks also to Dennis Slice for his helpful suggestions and for showing me his simulations demonstrating that the distribution of all possible triangles aligned to a reference was on a hemisphere. This work was supported in part by grants from the Systematic Biology (DEB 93-17572) and Ecological and Evolutionary Physiology (IBN-9728160) programs of the National Science Foundation. This paper is contribution no. 1042 from the Graduate Studies in Ecology and Evolution, State University of New York at Stony Brook.

Author's Address: F. James Rohlf, Department of Ecology and Evolution, State University of New York, Stony Brook, NY 11794-5245, USA; email: rohlf@life.bio.sunysb.edu

1. Introduction

The relatively new field of geometric morphometrics represents an important paradigm for the statistical study of variation and covariation of the shapes of biological structures. The notion of shape we are concerned with here is that of the relative positions of labeled points (corresponding to morphological landmarks in biology) in two-dimensional images or in the actual three-dimensional space of the organisms. The shape of a configuration of points may be represented by the coordinates of the points after the effects of variation in translation, rotation, and scale are removed. The analysis of the shapes of outlines are also part of geometric morphometrics but will not be considered here. Rohlf and Marcus (1993) give a general overview of the field and Bookstein (1991) supplies a detailed technical account. Marcus, Corti, Loy, Naylor, and Slice (1996) includes both introductory material and examples of applications to many fields of biology and medicine. The recent book by Dryden and Mardia (1998) gives a comprehensive coverage of shape statistics. The fundamental advances of geometric morphometrics over traditional approaches are in the way one measures the amount of difference between shapes, the elucidation of the properties of the multidimensional shape space defined by this metric, and the development of specialized statistical methods for morphometrics.

Traditional morphometric approaches are based on multivariate analyses of arbitrary collections of distance measures, ratios, and angles typically representing only part of the information that may be obtained from the positions of the landmarks on which these measurements are based. Those methods do not take into account information about the spatial relationships among the measured variables. Intuitively, one expects methods that take this additional information into account to have greater statistical power for detecting shape differences or covariation with other variables. Traditional methods only allow one to visualize such statistical relationships as scatter plots of numerical descriptors of shape, not as estimates of the shapes themselves, as is possible with the newer approaches.

Bookstein (1996a) points out that equivalent analyses of shape variation may be carried out using either coordinates of specimens aligned using generalized least-squares Procrustes analysis or by the use of matrices of partial warp scores. See Goodall (1991) or Rohlf and Slice (1990) for a discussion of Procrustes analysis and Bookstein (1991) or Rohlf (1993) for a discussion of partial warp scores. Each of these analyses is sufficiently complicated that software packages implementing these analyses have a number of options that control details of the way the analyses are performed. The choices may seem arbitrary unless one understands the relationships among the methods, and a user may find it difficult to decide which combinations of

options should be used. Walker (1996) and Rohlf, Loy, and Corti (1996) report on a number of empirical comparisons between analyses using coordinates of superimposed specimens, partial warp scores, and relative warp scores. The purpose of this paper is to show some of the relationships between these approaches and to indicate how these analyses should be implemented in order for the results to be compatible. Some new results on the geometry of shape space are presented and the advantages and disadvantages of alternative methods to analyze and depict shape differences are discussed.

2. Shape Comparisons and Shape Spaces

The data for a shape consists of a $k \times p$ matrix of coordinates, where p is the number of landmark points and k is the dimensionality of the physical space within which the objects are digitized. It is often convenient to treat the kp coordinates as a single row vector with kp elements. The order of the elements is arbitrary ($x_1,y_1,x_2,y_2,\ldots,x_p,y_p$ will be assumed). A sample of shapes may then be represented conveniently as a matrix with n rows and kp columns, i.e., as points in a kp-dimensional space, called a *figure space* by Goodall (1991).

A basic technique for comparing shapes is to superimpose them and then note the differences in the positions of the landmark points. The shapes are superimposed by first centering them on the origin so their means become zero and then scaling them to unit "centroid size" (square root of the sum of their squared coordinates, Bookstein 1991, pages 93-95). The coordinates of a shape treated as a single unit length vector with kp elements then corresponds to a point in *preshape space* (geometrically such points lie on the surface of a $k(p-1)$-dimensional hypersphere with unit radius). One of the shapes is then rotated to align it with the other so that d (the square root of the sum of squared differences between corresponding points) is as small as possible. The quantity d is often called a Procrustes distance, but there is a related quantity, ρ, to which this term is also applied (see below). Gower (1975) gives a general matrix algorithm to rotate one specimen to match another. Bookstein (1991, pages 262-265) gives an alternative, more efficient algorithm using complex regression but it is limited to two-dimensional coordinates. Procrustes distance was first used in the context of superimposition methods by Hurley and Cattell (1962) to measure agreement between two multivariate configurations of points. It was used by Sneath (1967) to measure the amount of difference between a pair of biological shapes. Cole (1996) surveys early uses of superimposition methods to study shape differences. Note that there are two important differences in the way in which superimpositions should be performed to compare shapes rather than multivariate

ordinations. When comparing multivariate ordinations it usually makes sense to reflect axes if it improves the fit because the orientation of axes are usually arbitrary. In morphometrics, reflections are not permitted because differences resulting from reflections are considered part of the overall shape difference (see Goodall 1991, and Rohlf 1996). Another difference is that in multivariate applications one wants to take advantage of the fact that one may achieve a better fit (smaller sum of squared deviations) by letting the centroid size of one configuration of points be reduced to $\cos(\rho)$ (ρ is defined below). Dryden and Mardia (1998), following Kent (1994), distinguish these two approaches and refer to the case where both objects are constrained to have unit centroid size as partial Procrustes fitting. When the size of one object is reduced to $\cos(\rho)$ it is called full Procrustes fitting. In this paper partial Procrustes fitting will be assumed. There has been some confusion, and many programs have ignored these distinctions.

Another fundamental operation is the computation of an average shape for a sample of specimens. The average may be defined as the shape whose sum of squared Procrustes distances to the other specimens is minimal. This measure is also the maximum likelihood estimate for the average shape in certain statistical models (Dryden and Mardia 1993; Kent 1994). It may be computed using what has been called generalized least-squares Procrustes superimposition method, GLS, as described by Gower (1975) and Rohlf and Slice (1990). This method is also called generalized Procrustes analysis, GPA, since it is not actually a generalized least-squares procedure. The iterative algorithm for this method aligns each specimen to a trial average shape and then estimates a new average as the average of the coordinates of the landmark points in these aligned specimens. For two-dimensional data the average may also be computed as the dominant eigenvector of a complex sums of squares and products matrix Kent (1994). Weighted means have also been proposed (Goodall 1991). The average configuration is usually scaled to have unit centroid size. It is often convenient to align the average configuration to its principal axes to give it a standard orientation.

The GLS method also produces a transformed dataset in which each specimen has been aligned to the average configuration. The matrix of aligned specimens has interesting geometric properties. Consider the case of $p = 3$ and $k = 2$ (i.e., triangles in the plane). Because $kp = 6$, each triangle may be represented by a point in a six-dimensional figure space (Goodall 1991). After a GLS alignment, the points only occupy a two-dimensional subspace of this space — the surface of a hemisphere in three dimensions (see Figure 1). The hemisphere has a unit radius because each aligned triangle is scaled to have a unit centroid size. The point at the pole of the hemisphere corresponds to the average triangle and is often called the reference.

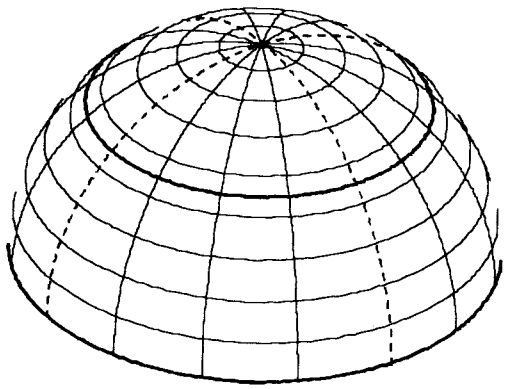

Figure 1. Preshape space of triangles aligned to a reference triangle. If the reference is an equilateral triangle then the bold co-latitude line (at an angle of $\pi/4$ from the pole) corresponds to the collinear triangles. The equator (at an angle of $\pi/2$ from the pole) corresponds to the single triangle that is the reflection of the reference triangle. Figure 2 shows a sequence of triangles corresponding to points along one of the dashed meridians.

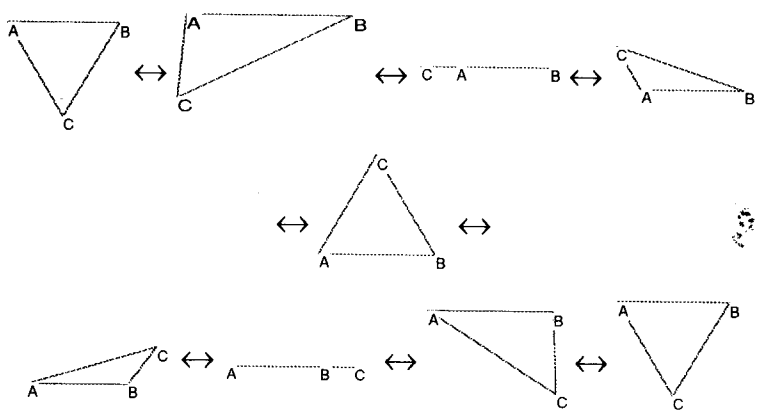

Figure 2. An example of a sequence of shapes corresponding to points along a meridian of the Hemisphere in Figure 1 (the meridian corresponds to the μ_1 axis in Figure 5). While any shape could be used as the pole, an equilateral triangle is illustrated here. Triangles correspond to angles of $-\pi/2$, $-\pi/3$ $-\pi/4$, $-\pi/6$ (top row), 0 (center), $\pi/6$, $\pi/4$, $\pi/3$, and $\pi/2$ (bottom row) from the axis of the hemisphere, i.e., points going from the equator at the left of the figure through the pole to the equator at the right. The points on the equator (the first and last shapes) correspond to the reflection of the triangle at the pole. In this example the two points at $\pi/4$ correspond to collinear triangles.

The surface of the hemisphere may be called the space of preshapes aligned with respect to the average shape. The full preshape space has no effects of rotation removed and corresponds to a three-dimensional space — the surface of a unit sphere in a four-dimensional space (Goodall 1991). The hemisphere is not the desired shape space because it has the wrong metric geometry (see below).

Triangles map to unique positions on the hemisphere except for the triangle that is most different from the triangle at the pole (it maps to the entire equator; see Figure 2). The Euclidean distance between the position of a shape on this hemisphere and the pole is equal to the partial Procrustes distance d_P discussed above. The distance from a full Procrustes fitting may be computed as $d_F = \sin(d_p)$. Because shapes correspond to points on a hemisphere with unit radius, it is natural to consider measuring distance as great circle distance, ρ (this is also the angle, in radians, between vectors from the center of the hemisphere to the two points being compared). Kendall (1984) showed that this was a Riemannian distance. The distances are related as $\rho = 2\sin^{-1}(d_p/2)$. Thus $d_F \leq d_p \leq \rho$. All have been called Procrustes distances. Following Dryden and Mardia (1993), they will be distinguished in this paper by the terms Procrustes distance (ρ), partial Procrustes chord distance (d_P), and full Procrustes chord distance (d_F).

Because the space of GLS aligned shapes corresponds to a hemisphere, it is clear that $0 \leq \rho \leq \pi/2$ for distances from the pole. The latitude lines are actually co-latitude lines because they are measured in angles from the pole rather than from the equator. The maximum value for ρ between any pair of shapes is $\pi/2$ (Kendall 1984). It might appear from Figure 1 that distances between shapes could be as large as π (for points approaching opposite sides of the equator) but that impression is misleading because the entire equator at $\pi/2$ actually corresponds to the same triangular shape (see Figure 2). Thus, this space does not accurately reflect Procrustes distances between pairs of shapes except when one member of the pair is the reference shape at the pole. If, for example, the shape at the pole corresponds to an equilateral triangle, then the solid co-latitude line at $\pi/4$ corresponds to all possible collinear triangles (all three vertices on the same line). Points beyond this co-latitude correspond to shapes that are closer to reflections of the equilateral reference shape. For $k = 2$ and $p > 3$ similar relationships hold but points corresponding to GLS aligned shapes lie on higher-dimensional hemispheres, and the equator no longer corresponds to a single shape because shapes maximally distant from the reference form a space of $p-3$ complex dimensions (Theorem 1 of Kendall 1984). For $k = 3$ the geometry is more complicated and will not be discussed here. Dryden and Mardia (1993) and Small (1996) address some of the properties of shape space for $k = 3$.

Many computer programs use full Procrustes fitting (e.g., GRF, Rohlf and Slice 1991, and GRFND, Slice 1993). Bookstein's (1991, pp. 262-265) method of alignment using complex regression also corresponds to a full Procrustes fitting. My "tps" series of programs (Rohlf 1998b; 1998c; 1998d) and "Morpheus et al." Software (Slice 1996) allow this choice among others. They are available from the www site

http://life.bio.sunysb.edu/morph

For small values of ρ, $\cos(\rho)$ is close to one and the distinction makes little difference. However, as ρ approaches its limit of $\pi/2$, $\cos(\rho)$ goes to zero. Figure 3 illustrates the result of re-scaling the space of triangles. The hemisphere of aligned triangles (Figure 1) becomes a sphere with a radius of 1/2 centered on (0,0,1/2). The equator of the hemisphere (the reflected reference) maps to a single point at the pole opposite the point corresponding to the reference, and the co-latitude line for collinear triangles becomes the equator of the sphere. Great circle distances along the surface of this sphere between all pairs of shapes (not just those involving the reference) are equal to 1/2 of their angular difference (in radians) on the sphere and are also equal to the Procrustes distance, ρ between the shapes. Thus the metric geometry of the surface of this sphere corresponds to Kendall's (1981, 1984) shape space for triangles. Figure 4 shows a cross-section through these two spaces. Although it does not correspond to a reasonable morphometric model, a reassuring result of Kendall (1984) is that if the vertices of a shape are independently and identically distributed spherical normal variables, then the distribution of shape is uniform in Kendall's shape space. Also important are the results of Small (1996, chapter 5) on the distribution of shapes.

For $k = 2$ and $p > 3$ similar relationships hold. GLS results in higher-dimensional hemispheres (still with unit radius). These higher-dimensional hemispheres cannot be transformed into Kendall's shape spaces by simply making radii equal to $\cos(\rho)$. The topology of shape space for $k = 3$ may be more complicated as there are situations that lead to cusps and folds in the space (but these correspond to what one might consider degenerate cases such as $p = 3$ or of having all the landmarks in a straight line). For $p > 3$ intuitive visualization is complicated by the fact that shape space is a complex projective space and no longer corresponds to a sphere (Kendall 1984). The geometry of this space has been worked out rigorously by Kendall (1981; 1984). He showed, for example, that shape space is a $kp - k - 1 - k(k-1)/2$-dimensional manifold ($2p - 4$ for 2D and $3p - 7$ for 3D). A manifold is a generalization to higher dimensions of a curved surface in three dimensions. Small (1996) gives an introduction to the topic and discusses applications to morphometrics.

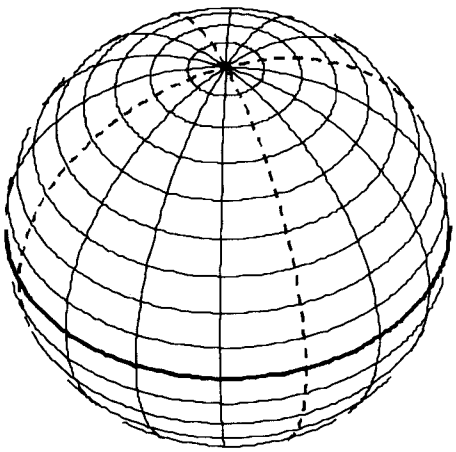

Figure 3. Kendall's shape space for triangles in the plane. The radius is equal to 1/2. The equator corresponds to the solid co-latitude line at $\pi/4$ in Figure 1. The South Pole corresponds to the equator in Figure 1. The dashed meridians correspond to those in Figure 2 and the u_1, u_2 axes in Figure 5.

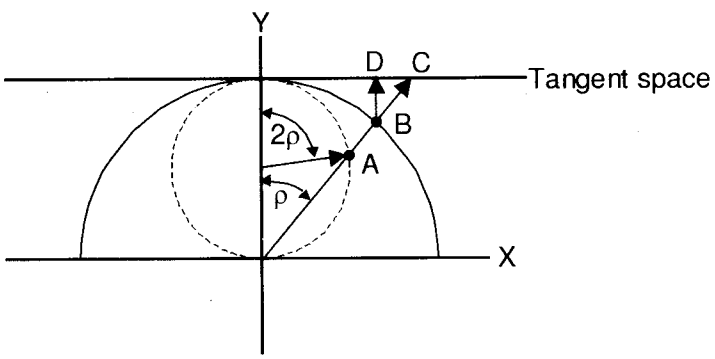

Figure 4. Diagram of a cross-section of a construction of Kendall's shape space for triangles (circle with a radius of 1/2), hemisphere of preshapes aligned to the reference (half circle with a radius of 1), and tangent space (tangent line). Procrustes distance is the angle ρ in radians. Point A represents the position of a shape in Kendall's shape space and B is the corresponding position in the hemisphere (yielding Procrustes tangent space coordinates). Point C is the stereographic projection of point A onto the tangent space (yielding stereographic shape coordinates) and D is the orthogonal projection of point B onto tangent space (yielding Kendall tangent space coordinates).

There have been other proposals for metrics for comparing shapes. These metrics lead to other shape spaces with quite different properties. Rohlf (1999a) compares these approaches by comparing their shape spaces implied for triangles in the plane.

3. Tangent Space

Special statistical methods (rather than the usual linear multivariate methods) are required to take into account the non-Euclidean geometry of Kendall's shape space for both two and three-dimensional landmarks. See Dryden and Mardia (1993, 1998), Goodall (1991), Goodall and Mardia (1993), Kent (1994), Mardia, Rabe and Kent (1995), Mardia and Dryden (1989a,b), and Small (1996) for work developing statistical methods for Kendall's shape space. When variation in shape is sufficiently small it is possible to make a good linear approximation to the space and then use standard multivariate methods (Kent 1994). The resulting space is of the same dimensionality as the shape space and may be viewed as tangent to it. The point of tangency corresponds to the reference shape (usually taken as an average shape). The projections of the points corresponding to the observed shapes are used for subsequent statistical analyses. A linear approximation will, of course, be best when the point of tangency is taken as close as possible to the positions of the points that will be used in an analysis. Surprisingly, this strategy is controversial. Several recent papers used references that could be near the periphery of the observed distribution or even outside it. For example, Zelditch, Bookstein, and Lundrigan (1992) used the shape of a juvenile when studying shape variation among adult cotton rats, Fink and Zelditch (1995), Zelditch and Fink (1995), and Zelditch, Fink, and Swiderski (1995) used an average juvenile of an outgroup species when studying adult piranhas, and Reis, Zelditch, and Fink (1998) used the average of the four smallest specimens.

Spaces tangent to Kendall's shape space have been constructed in two rather different ways in morphometrics. A stereographic projection has been used to map points from the surface of the shape space sphere to a tangent space. Stereographic projection is a standard tool for mapping points on the complex plane into a one-to-one correspondence with points on a sphere. The projection is the intersection of tangent space with a line that goes from the point antipodal to the reference through the point being projected (point C in Figure 4). Figure 3.2 in (Small 1996) also illustrates this point (note that in his diagram the reference is shown at the South Pole and the tangent space below the sphere). The coordinates of stereographic projections are called shape coordinates. Shapes close to the reference will map to points close to the origin, and the point antipodal to the reference maps to infinity. These

same projections may also be constructed by simply scaling each shape in the preshape space of shapes aligned with the reference (Figure 1) to have a centroid size of $1/\cos(\rho)$, where ρ is the its Procrustes distance to the reference. Figure 4 illustrates this relationship. In the past my "tps" series of programs (Rohlf 1998b; 1998c; 1998d) referred to this method as "$1/\cos(\rho)$ scaling."

Bookstein shape coordinates (Bookstein 1986) are well known and are a special case of a stereographic projection (Goodall 1991). They are usually constructed by mapping one vertex of a triangle, say A, to (0,0) and another, say B, to (1,0). The coordinates of the third vertex, C, are the Bookstein shape coordinates. Small (1996) maps vertex A to (-1,0), B to (1,0) and shows that these shape coordinates are equivalent to a stereographic projection using the collinear triangle with vertex C at (0,0) as the implied reference. Dryden and Mardia (1998) align vertices A and B to points at $(-1/2,0)$ and $(1/2,0)$. Bookstein shape coordinates work quite well when shape variation is small and vertices A and B are well separated (Rohlf 1999b). Different choices for the base of the triangle imply different reference triangles and thus lead to somewhat different results. One would prefer to use a reference that is close to the observed shapes, but Bookstein shape coordinates constrain the choice to one of three collinear triangles. Alternatively, one could explicitly select a reference corresponding to an average shape in the sample and use that for a general stereographic projection. For large variation in shape, the resulting shape coordinates have properties that need to be taken into consideration. For example, the projection of the average shape is not equal to the average of the projections. For small variation in shape, normally distributed variation around the average landmark position results in shape coordinates that are approximately normally distributed. See Small (1996) for further discussion of the properties of stereographic projections of shape space.

A tangent space may also be constructed by a projection of the hemisphere of preshapes aligned with respect to the average shape (as in Figure 1 for triangles) onto the space perpendicular to the direction corresponding to the reference (the axis of the hemisphere). Figure 5 shows the result for triangles. It is simply Figure 1 viewed from above. The projection may be computed as

$$\mathbf{X}' = \mathbf{X}(\mathbf{I}_{kp} - \mathbf{X}_c^t(\mathbf{X}_c\mathbf{X}_c^t)^{-1}\,\mathbf{X}_c)\,, \qquad (1)$$

where $\mathbf{X}$ is the $n \times kp$ matrix of aligned specimens (each with unit centroid size), $\mathbf{I}_{kp}$ is a $kp \times kp$ identity matrix, and $\mathbf{X}_c$ is the reference as a row vector of kp elements. Because $\mathbf{X}_c$ is usually scaled to unit centroid size, it is possible to simplify Equation (1) to $\mathbf{X}' = \mathbf{X}(\mathbf{I}_{kp} - \mathbf{X}_c^t\mathbf{X}_c)$. Matrix $\mathbf{X}'$ will be at most of rank $kp - k - 1 - k(k-1)/2$ (this is equal to 2 for triangles in the plane). In terms of Figure 1, the two nonsingular dimensions of $\mathbf{X}'$ correspond to a view

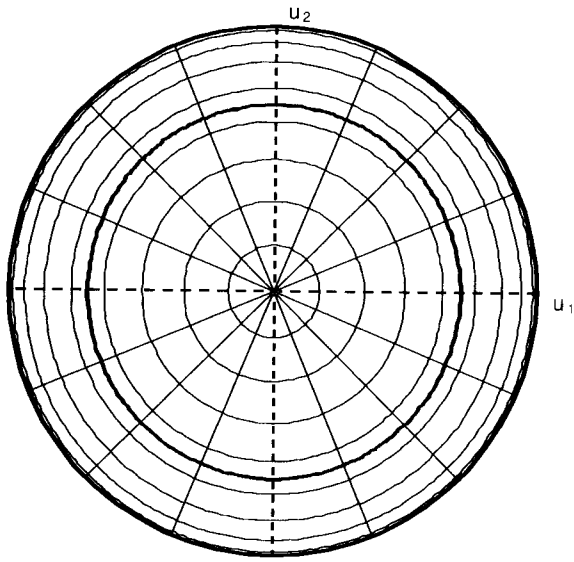

Figure 5. Kendall tangent space approximation to shape space. This space represents a projection of the preshape hemisphere of Figure 1 projected onto a tangent plane at the pole. The circles correspond to the co-latitude lines in Figure 1. The u_1 and u_2 axes (dashed lines) correspond to the dashed lines in Figure 1 and Figure 3 and to Bookstein's (1996b) linearized Procrustes estimates of the uniform component. The sequence of shapes in Figure 2 corresponds to points going from the left to the right end of the μ_1 axis.

from directly above the pole. Shapes close to the reference shape map to points near the origin in Figure 5 and shapes corresponding to points on the equator map to points on the circle with unit radius. Kent (1994) calls these aligned tangent projections. Dryden and Mardia (1993) call them Kendall tangent space coordinates (this latter term will be used in this paper). In the past my "tps" series of programs referred to this method (somewhat obscurely) as "shrunken $1/\cos(\rho)$ scaling." This projection has the desirable property that the projection of the average shape is equal to the average of the projected shapes. Kent (1994) suggests that one may use these shape variables in standard multivariate analyses if the data are concentrated in a relatively small region of shape space.

It is possible to transform Kendall tangent space coordinates for triangles to shape coordinates by simply dividing them by $(1-v^2)^{1/2}$, where v is the distance of the point from the origin in the Kendall tangent space. Note that as v approaches 1, shape coordinates approach infinity. The use of partial warp scores (with the linearized Procrustes estimate of the uniform

component included, see below) is an example of the implicit use of an orthogonal projection with the aligned shapes scaled to have unit centroid size. However, most studies using partial warp scores have used the $\cos(\rho)$ scaling described in the previous section. This practice is undesirable when shape variation is large because an orthogonal projection of a sphere confounds distinct shapes and this drawback does not simply correspond to ignoring reflections.

4. Is Shape Variation "Small"?

One of the first things to investigate in a practical application is whether the observed variation in shape is sufficiently small that the distribution of points in the tangent space may be used as a satisfactory approximation to their distribution in shape space. A direct method for answering this question is simply to plot Euclidean distances between all pairs of points in the tangent space against their Procrustes distances in shape space. Figure 7 below shows a typical example. One could also plot just the distances to the average shape, which would reduce the scatter to points along a curve, but it is useful to see the much larger distortion between the most distant pairs of shapes. An approximately linear relationship with a slope close to unity implies that one may satisfactorily use the tangent space to approximate shape space for these data.

The tpsSmall software (Rohlf 1998d), which performs these computations, has been made available for some time, and no one has reported a case in which the approximation seemed unsatisfactory. The only apparent exceptions were cases in which reflected specimens were inadvertently included. The fit was quite good once these specimens were properly reflected. (Rohlf 1996) conjectured that, at least in biological applications, the approximation would usually be good when there are more than just a few landmarks.

The effects of the different scaling choices discussed above are hard to distinguish empirically for the amount of shape variation usually encountered. However, orthogonal projections using $\cos(\rho)$ scaling results in slopes less than one, Kendall tangent space coordinates result in steeper slopes (slightly less than one), and shape coordinates result in slopes slightly greater than one.

5. Shape Variables

Most multivariate statistical analyses are performed using measurements on suites of variables rather than directly on points in a multidimensional space. There are several approaches one could take to generate variables from shape spaces. They may be defined a priori based on either some

Table 1. Shape variables based on the tangent space.

Projection	Shape coordinates	PCA scores
None	Procrustes tangent coordinates, **V**	**P**
Stereographic	Stereographic shape coordinates, **G**	**Q**
	Bookstein shape coordinates, **G′**	**Q′**
Orthogonal	Kendall tangent space coordinates, **V′**	**P′**
	Partial warp scores (including uniform component), **W′**	Relative warp scores, **P″**

aspect of the geometry of Kendall shape space or upon some theoretical model for the shapes being studied (Raup 1961, is a classic example of the latter). Alternatively, one may create variables based on the empirical patterns of variation found in a sample. Five such choices are discussed below. Table 1 gives a summary of the type of shape variables and some of the symbols used below.

1. *Stereographic shape coordinates* (stereographic projections, **G**, using a specified reference with Bookstein shape coordinates, **G′**, as a special case) provide a set of shape variables that span the $kp - k - 1 - \frac{1}{2}k(k-1)$-dimensional tangent space. Such coordinates correspond to point C in Figure 4. Goodall and Mardia (1992) and Dryden and Mardia (1993) describe a closely related approach based on a QR decomposition. Mardia and Dryden (1989a) give the exact joint distribution for Bookstein shape coordinates for small variation in shape (such as normally distributed digitizing error at each landmark). When variation is very small they find a normal approximation adequate. The interpretation of these shape variables depends on the choice of reference (or a baseline) and its orientation. Bookstein (1991) gives detailed instructions on how to interpret Bookstein shape coordinates to describe the implied changes in the shape of a triangle. A principal components analysis may be performed on the covariance matrix for **G** or **G′** to obtain a low-dimensional ordination, **Q** or **Q′** respectively, of the specimens. When sample sizes are greater than the number of shape variables, none of the eigenvalues is expected to be zero.

2. *Procrustes tangent space coordinates*, **V**, are the differences between the kp coordinates of the landmarks of the GLS aligned specimens (point B in Figure 4) and the reference. Such coordinates are computed as $\mathbf{V} = \mathbf{X} - \mathbf{1}_n\bar{\mathbf{X}}$,

where $\mathbf{X}$ is the $n \times kp$ matrix of aligned specimens scaled to unit centroid size, $\mathbf{1}_n$ a column vector of n ones, and $\bar{\mathbf{X}}$ a row vector containing the column averages of $\mathbf{X}$. The vector $\bar{\mathbf{X}}$ is proportional to the reference (its centroid size will be less than one because the preshape space is curved). These shape variables are not linearly independent because the effects of translation, size, and alignment to the reference have been removed. These singular dimensions must be taken into account in tests for group differences in shape using such standard multivariate methods as canonical variates, generalized T^2 tests, multivariate regression, or multivariate analysis of variance. These singularities are why Bookstein (1996a) states that "Procrustes residuals cannot lead to sound canonical variate analyses without modification." Software must make use of generalized inverses and proper adjustments to the various degrees of freedom to take into account the fact that there are fewer independent dimensions than there are shape variables. Note that while the overall tests of significance are invariant to rotation, the interpretation of a particular shape variable, say $1x$ (the displacement of landmark 1 in the x direction) depends on the orientation of the reference shape.

Because Procrustes tangent coordinates are redundant (more variables than dimensions) one may rotate them to their principal component axes and discard axes corresponding to zero eigenvalues. Doing so will lose no information about shape variation and will produce a dataset that may be analyzed using standard software because the covariance matrix is nonsingular. This practice also eliminates the dependence of the shape variables upon an arbitrary choice of orientation for the reference. The principal component projection scores are computed as $\mathbf{P} = \mathbf{VC}$, where $\mathbf{C}$ is the normalized matrix of eigenvectors of the $kp \times kp$ covariance matrix $\mathbf{S}$. Equivalently, one may compute $\mathbf{P}$ and $\mathbf{C}$ by performing the singular-value decomposition (Eckart and Young 1936; Jackson 1991) $\mathbf{V} = \mathbf{LDC}^t$, where $\mathbf{D}$ is the diagonal matrix of singular values (square roots of the eigenvalues of $\mathbf{S}$), $\mathbf{P} = \mathbf{LD}$, and $\mathbf{C}$ is the matrix of normalized eigenvectors as before.

There will be one more eigenvalue greater than zero than there are dimensions in the shape space because (despite their name) the points are in the preshape hemisphere of shapes aligned with respect to the reference rather than in the tangent space. The direction corresponding to the deviations from the tangent space (parallel to the reference) does not necessarily correspond to the last nonzero eigenvector of the covariance matrix and thus it cannot simply be ignored.

3. *Kendall tangent space coordinates*, $\mathbf{V}'$, are based on Procrustes tangent space coordinates and are computed as $\mathbf{V}' = \mathbf{X}' - \mathbf{1}_n\mathbf{X}_c$, where $\mathbf{X}'$ is the projection of points in the space of preshapes aligned with respect to the reference projected onto a space orthogonal to the reference (using Equation (1)), and $\mathbf{X}_c$ is the reference (the average scaled to unit centroid size). These

coordinates correspond to point D in Figure 4. As above, statistical analyses must take into account the fact that the covariance matrix will be singular. While most overall tests of significance are not affected, the interpretation of individual shape variables (coordinates) depends upon the orientation of the reference. One solution to both problems is to use projections onto principal component axes, computed as $\mathbf{P}' = \mathbf{V}'\mathbf{C}'$, where $\mathbf{C}'$ is the normalized matrix of eigenvectors of the $kp \times kp$ covariance matrix $\mathbf{S}'$ for the Kendall tangent space coordinates. There will be $\max\{kp - (n-1),\ k + 1 + 1/2k(k-1)\}$ of the eigenvalues equal to zero (at least four for 2D data and seven for 3D data). As before, discarding the corresponding eigenvectors will lose no information about shape variation and will eliminate the dependence of the shape variables upon an arbitrary orientation of the reference.

4. *Partial warp scores* (including the uniform component) are the basis for another approach (see Bookstein 1991, pages 326-328). These shape variables partition shape variation according to spatial scale. Shape variation may be partitioned into uniform (infinite scale) and non-uniform (local deformation) components. The former has $k - 1 + 1/2k(k-1)$ dimensions (2 for 2D and 5 for 3D data) and the latter $k(p-k-1)$ dimensions ($2p - 6$ for 2D and $3p - 12$ for 3D). The uniform component is best estimated using the linearized Procrustes method of (Bookstein 1996b). For two-dimensional data, the uniform component scores may be given by $\mathbf{U} = \mathbf{VT}$, where $\mathbf{V}$ is the matrix of Procrustes tangent space coordinates (see above),

$$\mathbf{T}^t = \begin{bmatrix} \sqrt{\frac{\alpha}{\lambda}}\,y_1 & \sqrt{\frac{\gamma}{\alpha}}\,x_1 & \sqrt{\frac{\alpha}{\lambda}}\,y_2 & \sqrt{\frac{\gamma}{\alpha}}\,x_2 & \cdots & \sqrt{\frac{\alpha}{\lambda}}\,y_p & \sqrt{\frac{\gamma}{\alpha}}\,x_p \\ -\sqrt{\frac{\gamma}{\alpha}}\,x_1 & \sqrt{\frac{\alpha}{\lambda}}\,y_1 & -\sqrt{\frac{\gamma}{\alpha}}\,x_2 & \sqrt{\frac{\alpha}{\lambda}}\,y_2 & \cdots & -\sqrt{\frac{\gamma}{\alpha}}\,x_p & \sqrt{\frac{\alpha}{\lambda}}\,y_p \end{bmatrix}, \quad (2)$$

and x and y are the coordinates of the landmarks in the reference (which has been aligned to its principal axes so that $\Sigma x_i y_i = 0$), $\alpha = \Sigma x_i^2$, and $\gamma = \Sigma y_i^2$). The matrix $\mathbf{U}$ has n rows and two columns. Of course, any rotation of $\mathbf{U}$ conveys the same information. The 3D case is somewhat more complicated and explicit equations have not yet been fully worked out (see Bookstein 1996b).

The non-uniform shape component may be decomposed using Bookstein's (1991) partial warps as shape variables. These are based on the thin-plate spline and are described in Bookstein (1991), Rohlf (1993), and Rohlf (1998a). This spline is used to represent shape differences as a smooth deformation of a reference shape into another shape. Scores (projections) for these variables are computed as the $n \times k(p-k-1)$ matrix

$$\mathbf{W} = \mathbf{V}(\mathbf{E} \otimes \mathbf{I}_k)\,, \quad (3)$$

where $\mathbf{E}$ contains the first $p - k - 1$ columns of the matrix of normalized

eigenvectors of the bending energy matrix, $\mathbf{I}_k$ is a $k \times k$ identity matrix, and $\otimes$ is the Kronecker tensor product operator. The order of operations differs from that given in Rohlf (1993) because it was assumed there that all the x coordinates were given first followed by the y coordinates. The bending energy matrix is the upper left $p \times p$ block of $\mathbf{L}^{-1}$, where $\mathbf{L}$ is a $(p + k + 1) \times (p + k + 1)$ matrix that is a function of the reference and is defined in Bookstein (1991).

The **U** and **W** matrices are orthogonal to each other. Together,

$$\mathbf{W}' = (\mathbf{W} \mid \mathbf{U}), \tag{4}$$

they have $kp - k - 1 - 1/2k(k-1)$ columns ($2p - 4$ for 2D) which span the tangent space. Even though there are no redundant dimensions, one may still wish to perform a principal components analysis to express most of the variation using a few derived variables. Bookstein (1989) calls this strategy an analysis of relative warps. Let

$$\mathbf{P}'' = \mathbf{W}'\mathbf{C}'', \tag{5}$$

where $\mathbf{C}''$ is the normalized eigenvector matrix of the covariance matrix based on $\mathbf{W}'$. Note that (Rohlf 1993) introduced a parameter α that allows one to weight shape differences according to spatial scale (only the equal weighting case, $\alpha = 0$, will be considered here). Rohlf et al. (1996) is an example of performing a variety of shape analyses using multivariate analyses based on **W**, **U**, $\mathbf{W}'$, and other matrices.

5. *A priori shape variables* represent another approach. Rather than using **W** and **U** matrices based on a model of deformation of thin metal plates, one could use any set of orthogonal vectors that span the tangent space. They could represent contrasts among variables of interest to the investigator. One might, for example, wish to contrast variation within and among certain groups of landmarks.

6. Comparison of Shape Variables

While there are distinct differences among the methods described above, one should keep in perspective the fact that for the amount of variation in shape normally found in biological data, they usually lead to very similar statistical conclusions. Rohlf (1999b) compares these and other morphometric methods in terms of their type I error levels and their power for distinguishing different types of shape differences.

Stereographic shape coordinates represent a somewhat extreme nonlinear projection of shape space unless the points are close to the reference (which is usually difficult to achieve using Bookstein shape coordinates). Dryden and Mardia (1993) observe that a principal components analysis of Bookstein shape coordinates may imply strong dimensions of shape

variability when variation at each landmark is actually independent. This observation holds for stereographic shape coordinates in general unless the reference is taken as a shape close to the average. One may visualize the reason for this problem for triangular shapes by the fact that a uniform circular scatter of points on a sphere (corresponding to uncorrelated variation around an average shape) will not project to a uniform circular scatter in tangent space using a stereographic projection unless the circle is centered at the reference. Because a stereographic projection is conformal, a circular equal frequency contour will map to a circle in tangent space (McCleary 1994). However, concentric circles do not map to concentric circles because the transformation skews distributions away from the origin. Dryden and Mardia (1993) suggest that this structural correlation will not be present for Procrustes tangent space coordinates or Kendall tangent space coordinates (because their distribution will be centered on the reference shape). However, their distribution also becomes quite distorted for mean shapes far from the reference. Another obvious problem with stereographic shape coordinates is that the variance is inflated for shapes further from the reference.

When shape variation is small, the differences between Procrustes tangent space coordinates and Kendall tangent space coordinates are very small. However, Procrustes tangent space coordinates include what should be considered a spurious dimension results from the curvature of shape space. Kendall tangent space coordinates are just Procrustes tangent space coordinates with this uninformative dimension removed by an orthogonal projection. Their only problem is that they are redundant but, as shown above, the singular dimensions are easily removed.

Matrices $\mathbf{V}'$, $\mathbf{P}'$, and $\mathbf{W}'$ contain the same information about shape variation and give the same distances between shapes, and thus most standard multivariate statistical analyses (i.e., those invariant to linear transformations of the variables) will give equivalent tests of significance. This result may be demonstrated as follows. The projections of the shapes onto their principal component axes in the tangent space (see above) are $\mathbf{P}'' = \mathbf{W}'\mathbf{C}''$. Using the relationships from Equations (4) and (5),

$$\mathbf{W}' = \mathbf{V}[\mathbf{E} \otimes \mathbf{I}_k \mid \mathbf{T}], \text{ so that} \tag{6}$$

$$\mathbf{P}'' = \mathbf{V}[\mathbf{E} \otimes \mathbf{I}_k \mid \mathbf{T}]\mathbf{C}''. \tag{7}$$

$\mathbf{P}''$ is also equal to $\mathbf{V}'[\mathbf{E} \otimes \mathbf{I}_k \mid \mathbf{T}]\mathbf{C}''$ because $\mathbf{X}_c$ is orthogonal to both the uniform and the non-uniform shape components ($\mathbf{X}_c\mathbf{E} = \mathbf{X}_c\mathbf{T} = 0$ and $[\mathbf{E} \otimes \mathbf{I}_k \mid \mathbf{T}] = (\mathbf{I} - \mathbf{X}_c^t(\mathbf{x}_c\mathbf{X}_c^t)^{-1})\,[\mathbf{E} \otimes \mathbf{I}_k \mid \mathbf{T}]$). Finally, we replace $\mathbf{V}'$ with its PCA decomposition, $\mathbf{V}' = \mathbf{P}'\mathbf{C}'^t$, to obtain

$$\mathbf{P}'' = \mathbf{P}'\mathbf{C}'^t[\mathbf{E} \otimes \mathbf{I}_k \mid \mathbf{T}]\,\mathbf{C}''. \tag{8}$$

Thus, $\mathbf{P}''$ is equal to $\mathbf{V}'$ or $\mathbf{P}'$ post-multiplied by the product of matrices whose columns are orthogonal and of unit length. In fact, $\mathbf{P}'' = \mathbf{P}'$ because principal component scores are invariant to rotations of the variables on which they are based. Geometrically, $\mathbf{V}'$ (Kendall tangent space coordinates), $\mathbf{P}'$ (their principal components), $\mathbf{W}'$ (partial warp scores), and $\mathbf{P}''$ (relative warp scores) differ only by a rotation. Thus statistics and multivariate tests of significance which are invariant to rotation (e.g., principal components, multivariate analysis of variance, canonical variates analysis, D^2, etc.) will give the same overall results.

On the other hand, using stereographic projections, $\mathbf{G}$, will yield different results (even though it contains the same information) because it represents a nonlinear transformation of shape space. Ordinations, $\mathbf{Q}$ and $\mathbf{Q}'$, will yield different results unless the reference used for computing $\mathbf{G}$ is the same as that implied by the use of Bookstein shape coordinates.

The method of using *a priori* shape variables may be viewed as simply another rotation of Kendall tangent space coordinates if the shape variables are orthogonal to each other and to the reference. Such variables would have the advantage of an *a priori* interpretation, but it may be very difficult to construct biologically interesting variables that still satisfy these constraints.

7. Recovery of Shapes from Tangent Space

Conventional multivariate statistical analyses provide both tests of significance and various plots that allow one to visualize the patterns of variation and covariation in a dataset — at least to the extent that they are adequately summarized in a few dimensions. Multivariate analyses of shape variables allow additional visualizations — the depiction of the actual shapes corresponding to points in the multivariate spaces. This option is possible because a shape maps to a unique position in the tangent space. For those multivariate analyses that correspond to simply rotating and possibly dilating the tangent space it is easy to determine the inverse transformation back to shape space. In those analyses that include a projection into a lower-dimensional space (e.g., when one retains only the first few PCA or CVA axes) some information is lost. An approximation is to assume that the projection of a shape onto the discarded dimensions is zero.

One of the simplest applications is to display the shape corresponding to the average of a group of specimens. An illustration of a shape is usually very helpful to a researcher. This observation is especially true when the shape variables are mathematically constructed variables such as partial warp or relative warp scores that are hard to visualize intuitively. To plot a shape one must be able to transform a point in the space of shape variables back to a point in shape space (expressed as coordinates of landmarks for an object

centered on the reference and scaled to unit centroid size). The computational steps depend, of course, on the shape variables being used.

If the shape variables are Kendall tangent space coordinates, then one only needs to project back onto the preshape hemisphere of shapes aligned with respect to the reference using the relationship

$$\mathbf{X} = \mathbf{V}' + \cos(\rho)\mathbf{X}_c\,, \tag{9}$$

where $\mathbf{V}'$ is a matrix of coordinates of points in the tangent space and ρ is the Procrustes distance from the shape to the reference. Because $\cos(\rho)$ is usually just slightly less than 1 and $\mathbf{V}'$ is approximately a deviation of an aligned shape from the reference, we are approximately just adding the reference back in.

If the shape variables correspond to transformations of $\mathbf{V}'$ then the inverse of that transformation must be applied to visualize the corresponding shape. For a principal components analysis of $\mathbf{V}'$ we have the relationship

$$\mathbf{X} = \mathbf{P}'\,\mathbf{C}'^{-1} + \cos\rho)\mathbf{X}_c\,. \tag{10}$$

Because $\mathbf{C}'$ is orthonormal, $\mathbf{C}'^{-1} = C't$. In practice only the first few columns of $\mathbf{C}'$ are retained. The projections on the ignored dimensions are taken as zero. If partial warps are used as shape variables the relationship is

$$\mathbf{X} = \mathbf{W}'\,(\mathbf{E} \otimes \mathbf{I}_k \mid \mathbf{T})^{-1} + \cos(\rho)\mathbf{X}_c\,. \tag{11}$$

The columns of $(\mathbf{E} \otimes \mathbf{I}_k \mid \mathbf{T})$ are orthogonal and of unit length. Similarly for a principal components analysis of the partial warps (i.e., an analysis of relative warps, Bookstein 1991; Rohlf 1993)

$$\mathbf{X} = \mathbf{P}''\,\mathbf{C}''^{-1} + \cos(\rho)\mathbf{X}_c\,. \tag{12}$$

Because $\mathbf{C}''$ is orthonormal, $\mathbf{C}''^{-1} = \mathbf{C}''^{t}$.

Once one may display the shape corresponding to a point, many other types of useful visualization tools are possible — especially using interactive software. One may, for example, display the shape corresponding to any point in a PCA ordination (as done in the tpsRelw software, Rohlf 1998c). Another important application is in regression analysis, where one may visualize the results of a multivariate regression by displaying predicted shapes corresponding to variation in independent variables (as done in the tpsRegr software, Rohlf 1998b). One may also investigate allometry (the change of shape as a function of size) by visualizing variation as a function of size. Size may also be incorporated in the visualizations by including size as a scale factor.

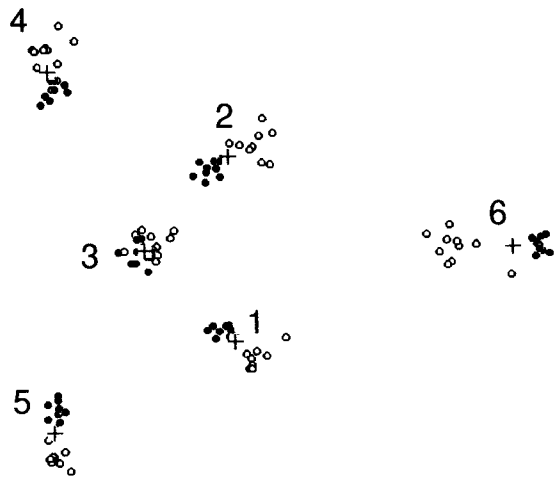

Figure 6. GLS superimposition for the simulated dataset from Rohlf and Slice (1990). The two groups are indicated by the open and filled circles and the consensus configuration is shown by the + signs. The specimens were sampled from two populations differing only in the average position of landmark 6 (even though the GLS results show appreciable differences at all landmarks except the central one).

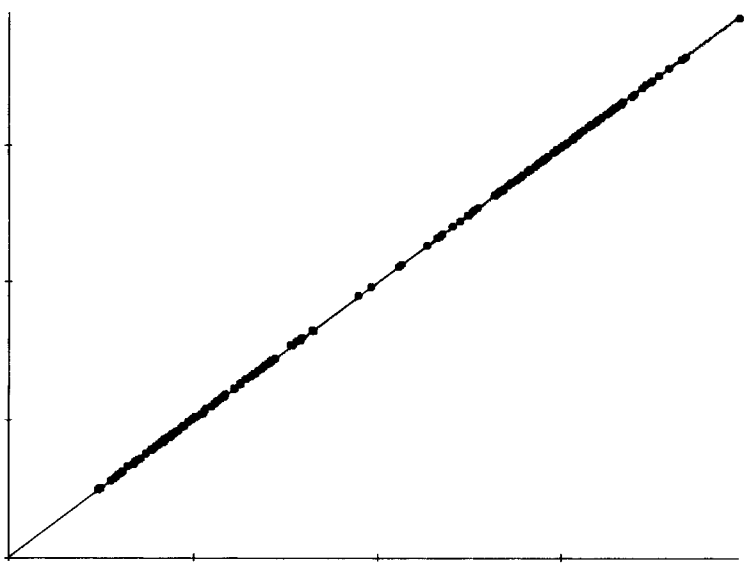

Figure 7. Plot of Euclidean distances , d, in the tangent space against Procrustes distance, ρ, in shape space for the data in Figure 6. Tic marks correspond to 0.1 units (the largest possible) ρ is $\pi/2 \approx 1.5708$. The slope (through the origin) is 0.996438 and the uncentered correlation is 0.999998. Plot generated by the tpsSmall software (Rohlf 1998d).

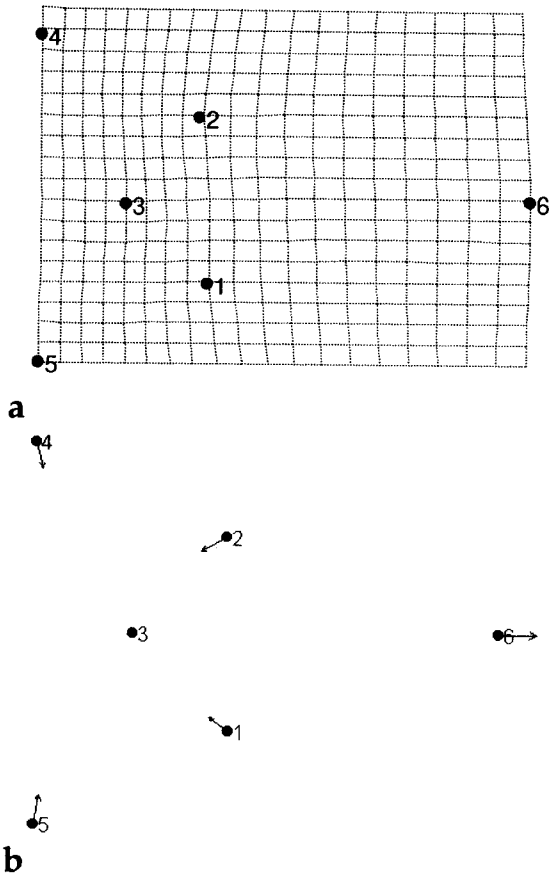

Figure 8. Representations of shape differences between the average specimen and the average of the sample from the second population. a. The difference between the average shape and mean of the second population is shown as a thin-plate spline. If there were no shape difference all the cells would be squares of the same size. b. The same shape difference shown as displacements at each landmark, Figure prepared using the tpsRegr (Rohlf 1998b).

8. An Example

It is difficult to compare the methods using real datasets because very similar results are expected for the relatively small levels of variation in shape found in most applications of morphometrics to biology and medicine. Thus, somewhat exaggerated artificial datasets may be helpful. Figure 1 of Rohlf and Slice (1990) is a simple example. There are 10 specimens sampled from each of two populations. Each specimen has six two-dimensional landmarks. Figure 6 shows the GLS superimposition of all the specimens with the members of the two groups identified. Tests for group differences using

canonical variates analysis (CVA) will be compared using different shape variables. A T^2-test could also have been used and would have yielded an equivalent test of significance for the difference in average shapes.

First, an average shape was computed using GLS, the specimens were then aligned to this reference, scaled to unit centroid size, and then projected onto the space orthogonal to the consensus configuration to construct Kendall tangent space coordinates (point D in Figure 4). Figure 7 shows Euclidean distances in the tangent space plotted against Procrustes distances. As usual, the correlation is very high and thus it seems safe to use the tangent space to approximate the nonlinear shape space.

Bookstein shape coordinates, $\mathbf{G}'$, were computed using landmarks 3 and 6 as a baseline (Figure 8 provides identifying numbers for the landmarks). The transformed coordinates of the other landmarks were used as eight variables in a CVA to test for differences between the two known groups. The resulting Wilks's lambda value was 0.02210562 ($P = 5.12 \times 10^{-8}$).

The twelve Kendall tangent space coordinates from the GLS were then used as variables in a CVA to test for differences between the two groups. Because these $kp = 12$ variables actually provide information on variation only in the $2p - 4 = 8$-dimensional tangent space, the pooled within-groups covariance matrix must be singular. The NTSYSpc software (Rohlf 1997) was used because its CVA program ignores dimensions with variation smaller than a user-specified threshold by performing a CVA using PCA scores based on the pooled within-groups covariance matrix. The eighth eigenvalue of the pooled covariance matrix was 0.00008594. Eigenvalues 9 through 12 were effectively zero (less than 10^{-19}) and were thus ignored by the program. The resulting Wilks's lambda value was equal to 0.01941165 ($P = 2.52 \times 10^{-8}$). As expected, this value was not the same as that obtained using Bookstein shape coordinates.

The GLS aligned specimens scaled to unit centroid size were then used to compute the 20×6 matrix of partial warp scores. The linearized Procrustes estimates of uniform shape component (equations given above) were appended as two additional columns to yield a 20×8 matrix, $\mathbf{W}'$, corresponding to a rotation of Kendall tangent space coordinates within the tangent space. The $\mathbf{W}'$ matrix was then used in a CVA. Standard software may be used in this case because the covariance matrix is expected to be of full rank. The value for Wilks's lambda, 0.01941167, only differed from the previous result in the eighth decimal place (rounding error). Finally, an analysis of relative warps with $\alpha = 0$ and the uniform component included was performed on the same data. The resulting 20×8 matrix of relative warp scores was again analyzed by CVA. The Wilks's lambda was again equal to 0.01941167. Thus identical significance tests were obtained using Kendall

tangent space coordinates, partial warp scores, and relative warp scores. The ordination plots using the canonical variate axes would also be the same but are not shown because there are only two groups. The implied shape differences between the two groups are also the same for the different analyses even though they are described using different shape variables.

Figure 8 shows the differences between the consensus configuration and the second of the two groups both as a deformation of the average shape (using a thin-plate spline) and as landmark displacements (using vectors). The spline shows quite clearly that the region to the right is expanded in the second group compared to the first. The vectors seem to imply a more complicated shape change. Properly interpreted, they describe the identical shape difference. The resistant fit superimposition method (Rohlf and Slice 1990) is a tool that may be useful when, as in the present example, most of the shape differences can be explained as displacements in just a few landmarks. In such cases, this method may make the shape differences very obvious (see Figure 9).

9. Discussion

Because the methods discussed above are based on a least-squares alignment of shapes, an understanding of the metric geometry of the space of shapes aligned with the reference is important. Two rather different approaches to constructing tangent space approximation were described (stereographic projections of shape space and an orthogonal projection of preshapes aligned to the reference). Which should be used in practical applications? As in the artificial example in the previous section, it usually will make little difference in most applications because shape variation is usually relatively small (especially when there are more than just a few landmarks). However as shape variation gets larger the approximation seems to become worse for stereographic shape coordinates. This observation is especially true when they are not tangent at the reference, as is usually the case with Bookstein shape coordinates.

If one uses the orthogonal projection approach, should one use Kendall tangent space coordinates or various shape variables derived from them such as partial warps? As demonstrated above, for overall tests of significance it does not matter, unless one would like to interpret the shape variables themselves. Kendall tangent space coordinates have the advantage of simplicity — they are directly related to the landmark displacements estimated by the superimposition of each shape onto the reference. However they tend to be highly correlated in part because they are not linearly independent (their covariance matrix has eigenvalues equal to zero). Thus, they should not be interpreted separately for each landmark.

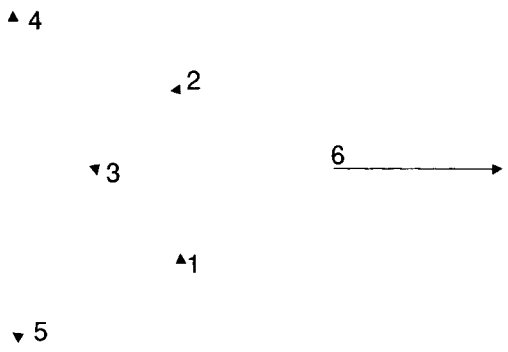

Figure 9. Differences in shape between the two groups shown as displacement vectors at each landmark (as in Figure 8b) but after superimposition using the resistant fit method. Except for landmark 6, the vectors are shorter than the arrowheads. This is consistent with the populations differing only in the relative position of landmark 6.

Although they are geometrically orthogonal, partial warps are usually highly correlated. Still, the idea of partitioning shape variation into components at different spatial scales is attractive. In some applications it may be interesting to know whether differences are mostly at larger or at smaller spatial scales. One could also delete a component if one thought there were distortions in the specimens at a certain spatial scale. For example, one could leave out the uniform shape component if the specimens seemed to be deformed uniformly (similar to the effects of the retro-deforming method of Motani 1997). Unfortunately, many papers try to name and interpret each partial warp. There are several problems with this practice. First, the partial warps are a priori defined functions based solely of the geometry of the reference configuration. It is unlikely that functions that do not take into account covariation in the data will happen to align with some interesting pattern in the data. The decomposition is based on a model for the deformation of a thin metal plate — not a model from biology or some other application area. Another problem is that slight changes in the reference may cause a rotation of the partial warps and thus change their meaning (Rohlf 1998a). The addition of a landmark may change what was an infinite scale uniform shape change into a local deformation. Thus, it is unlikely that the partial warp axes themselves (except for perhaps at the largest and smallest scales) correspond to any interesting underlying causal variables.

An important distinction among the methods is in how one wishes to display shape differences. One may show differences as vector displacements at each landmark or as deformations using the thin-plate spline. To describe the results of the former analysis, one would discuss apparent displacements

of landmarks. For the latter, one would describe differences using terms such as regions of expansion, bending, etc. However, the two representations contain the same information and suggest the same shape differences and thus are interchangable. One needs to visualize the implication of all the displacement vectors simultaneously (which is not always easy). An obvious example of the problem is shown in Figure 8a where there is a large difference in the position of one landmark yet the GLS superimposition in Figure 8b shows apparent displacements across most of the landmarks. This well-known property of least-squares superimposition was the reason for the development of the resistant fitting method (Siegel, 1982, Rohlf and Slice, 1990) illustrated in Figure 9. The thin-plate spline seems more effective in showing the overall differences between shapes. Such deformation plots are easily prepared using partial warp scores (see Rohlf 1993).

References

BOOKSTEIN, F. L. (1986), "Size and Shape Spaces for Landmark Data in Two Dimensions (with discussion and rejoinder)," *Statistical Science, 1*, 181-242.

BOOKSTEIN, F. L. (1989), "Principal Warps: Thin-Plate Splines and the Decomposition of Deformations," *Institute of Electrical and Electronics Engineers, Transactions on Pattern Analysis and Machine Intelligence, 11*, 567-585.

BOOKSTEIN, F. L. (1991), *Morphometric Tools for Landmark Data: Geometry and Biology*, New York: Cambridge University Press.

BOOKSTEIN, F. L. (1996a), "Combining the Tools of Geometric Morphometrics," in *Advances in Morphomtrics, Vol. 284*, Eds., L.F. Marcus, M. Corti, A. Loy, G.J.P. Naylor, and D. E. Slice, New York: Plenum, 131-151.

BOOKSTEIN, F. L. (1996b), "A Standard Formula for the Uniform Shape Component in Landmark Data," in *Advances in Morphometrics, Vol. 284*, Eds., L.F. Marcus, M. Corti, A. Loy, G.J.P. Naylor, and D. E. Slice, New York: Plenum, 153-168.

COLE, T. M., III. (1996), "Historical Note: Early Anthropological Contributions to "Geometric Morphometrics"," *American Journal of Physical Anthropology, 101*, 291-296.

DRYDEN, I. L., and MARDIA, K. V. (1993), "Multivariate Shape Analysis," *Sankhya, 55*, 460-480.

DRYDEN, I. L., and MARDIA, K. V. (1998), *Statistical Shape Analysis*, New York: Wiley.

ECKART, C., and YOUNG, G. (1936), "The Approximation of One Matrix by Another of Lower Rank," *Psychometrika, 1*, 211-218.

FINK, W. L., and ZELDITCH, M. L. (1995), "Phylogenetic Analysis of Ontogenetic Shape Transformations: A Reassessment of the Piranha Genus *Pygocentrus* (Teleostei)," *Systematic Biology, 44*, 344-361.

GOODALL, C. R. (1991), "Procrustes Methods in the Statistical Analysis of Shape (with discussion and rejoinder)," *Journal of the Royal Statistical Society, Series B, 53*, 285-339.

GOODALL, C. R., and MARDIA, K. V. (1992), "The Noncentral Bartlett Decompositions and Shape Densities," *Journal. Multivariate Analysis, 40*, 94-108.

GOODALL, C. R., and MARDIA, K. V. (1993), "Multivariate Aspects of Shape Theory," *Annals of Statistics, 21*, 848-866.

GOWER, J. C. (1975), "Generalized Procrustes Analysis," *Psychometrika, 40*, 33-51.

HURLEY, J. R., and CATTELL, R. B. (1962), "The Procrustes Program: Producing a Direct Rotation to Test an Hypothesized Factor Structure," *Behavioral Science, 7*, 258-262.

JACKSON, J. E. (1991), *A User's Guide to Principal Components*, New York: Wiley.

KENDALL, D. G. (1981), "The Statistics of Shape," in *Interpreting Multivariate Data*, Ed., V. Barnett, New York: Wiley, 75-80.

KENDALL, D. G. (1984), "Shape-Manifolds, Procrustean Metrics and Complex Projective Spaces," *Bulletin of the London Mathematical Society, 16*, 81-121.

KENT, J. T. (1994), "The Complex Bingham Distribution and Shape Analysis," *Journal Royal Statistical Society, B, 56*, 285-299.

MARCUS, L. F., CORTI, M., LOY, A., NAYLOR, G.J.P., and SLICE, D. E. (1996), *Advances in Morphometrics*, New York: Plenum.

MARDIA, K. V., and DRYDEN, I. L. (1989a), "Shape Distributions for Landmark Data," *Advances Applied Probability, 21*, 742-755.

MARDIA, K. V., and DRYDEN, I. L. (1989b), "The Statistical Analysis of Shape Data," *Biometrika, 76*, 271-281.

MARDIA, K. V., RABE, S., and KENT, J. T. (1995), "Statistics, Shape and Images," in *Complex Stochastic Systems and Engineering*, Ed., D.M. Titterington, Oxford: Clarendon Press, 85-103.

MCCLEARY, J. (1994), *Geometry from a Differentiable Viewpoint*, New York: Cambridge Press.

MOTANI, R. (1997), "New Technique for Retrodeforming Tectonically Deformed Fosils, with an Example for Ichthyosaurian Specimens," *Lethaia, 30*, 221-228.

RAUP, D. M. (1961), "The Geometry of Coiling in Gastropods," *Proceedings of the National Academy of Science, 47*, 602-609.

REIS, R. E., ZELDITCH, M. L., and FINK, W. L. (1998), "Ontogenetic Allometry of Body Shape in the Neotropical Catfish Callichthys (Teleostei: Siluriformes)," *Copeia, 1998*, 177-182.

ROHLF, F. J. (1993), "Relative Warp Analysis and an Example of Its Application to Mosquito Wings," in Contributions to Morphometrics, Eds., L. F. Marcus, E. Bello, and A. Garcia-Valdecasas, Madrid: Museo Nacional de Ciencias Naturales, 131-159.

ROHLF, F. J. (1995), "Multivariate Analysis of Shape Using Partial-Warp Scores," in *Proceedings in Current Issues in Statistical Shape Analysis*, Eds., K.V. Mardia and C.A. Gill, Leeds: University of Leeds, 154-158.

ROHLF, F. J. (1996), "Morphometric Spaces, Shape Components and the Effects of Linear Transformations," in *Advances in Morphometrics, Vol. 284*, Eds., L.F. Marcus, M. Corti, A. Loy, G.J.P. Naylor, and D.E. Slice, New York: Plenum, 117-129.

ROHLF, F. J. (1997), "NTSYS-pc: Numerical Taxonomy and Multivariate Analysis System," Exeter Software, Setauket, New York.

ROHLF, F. J. (1998a), "On Applications of Geometric Morphometrics to Studies of Ontogeny and Phylogeny," *Systematic Biology, 47*, 147-158.

ROHLF, F. J. (1998b), "tpsRegr: Shape Regression," Department of Ecology and Evolution, State University of New York at Stony Brook, Stony Brook, New York.

ROHLF, F. J. (1998c), "tpsRelw: Analysis of Relative Warps," Department of Ecology and Evolution, State University of New York at Stony Brook, Stony Brook, New York.

ROHLF, F. J. (1998d), "tpsSmall: Is Shape Variation Small?" Department of Ecology and Evolution, State University of New York at Stony Brook, Stony Brook, New York.

ROHLF, F. J. (1999a), "On the Use of Shape Spaces to Compare Morphometric Methods," *Hystrix, 00*, to appear.

ROHLF, F. J. (1999b), "Statistical Power Comparisions Among Alternative Morphometric Methods.," *American Journal of Physical Anthropology*, in press.

ROHLF, F. J., LOY, A., and CORTI, M. (1996), "Morphometric Analysis of Old World Talpidae (Mammalia, Insectivora) Using Partial Warp Scores," *Systematic Biology, 45*, 344-362.

ROHLF, F. J., and MARCUS, L. F. (1993), "A Revolution in Morphometrics," *Trends in Ecology and Evolution, 8*, 129-132.

ROHLF, F. J., and SLICE, D. E. (1990), "Extensions of the Procrustes Method for the Optimal Superimposition of Landmarks," *Systematic Zoology, 39*, 40-59.

ROHLF, F. J., and SLICE, D. E. (1991), "GRF - Generalized Rotational Fit Methods," Department of Ecology and Evolution, State University of New York at Stony Brook, Stony Brook, New York.

SIEGEL, A. F. (1982), "Robust Regression Using Repeated Medians," *Biometrika, 69*, 242-244.

SLICE, D. E. (1993), "GRF-ND: Generalized Rotational Fitting of N-dimensional Data," Department of Ecology and Evolution, State University of New York at Stony Brook, Stony Brook, New York.

SLICE, D. E. (1996), "Morpheus et al.: Multiplatform Software from Morphometric Analysis," Department of Ecology and Evolution, State University of New York at Stony Brook, Stony Brook, New York.

SMALL, C. G. (1996), *The Statistical Theory of Shape*, New York: Springer.

SNEATH, P. H. A. (1967), "Trend-Surface Analysis of Transformation Grids," *Journal of Zoology, London, 151*, 65-122.

WALKER, J. A. (1996), "Principal Components of Body Shape Variation Within an Endemic Radiation of Stickleback," in *Advances in Morphometrics*, Eds., L.F. Marcus, M. Corti, A. Loy, G.J.P. Naylor, and D. E. Slice, New York: Plenum Press, 321-334.

ZELDITCH, M. L., BOOKSTEIN, F. L., and LUNDRIGAN, B. L. (1992), "Ontogeny of Integrated Skull Growth in the Cotton Rat *Sigmodon fulviventer*," *Evolution, 46*, 1164-1180.

ZELDITCH, M. L., and FINK, W. L. (1995), "Allometry and Developmental Integration of Body Growth in a Piranha, *Pygocentrus nattereri* (Teleostei: Ostariophysi)," *Journal of Morphology, 223*, 341-355.

ZELDITCH, M. L., FINK, W. L., and SWIDERSKI, D. L. (1995), "Morphometrics, Homology, and Phylogenetcs: Quantified Characters as Synapomorphies," *Systematic Biology, 44*, 179-189.